Photochemistry and Photobiology, 2020, 96: 349–357

Synthesis and Characterization of Ru(II) Complexes with π-Expansive Imidazophen Ligands for the Photokilling of Human Melanoma Cells†

Goutam Ghosh[1,2], Huimin Yin[1], Susan M.A. Monro[1], Tariq Sainuddin[1], Lloyd Lapoot[2,3], Alexander Greer*[2,3] and Sherri A. McFarland*[1,4,5]

[1]Department of Chemistry, Acadia University, Wolfville, NS, Canada
[2]Department of Chemistry, Brooklyn College of the City University of New York, Brooklyn, NY
[3]Ph.D. Program in Chemistry, The Graduate Center of the City University of New York, New York, NY
[4]Department of Chemistry and Biochemistry, The University of North Carolina at Greensboro, Greensboro, TX
[5]Department of Chemistry and Biochemistry, The University of Texas at Arlington, Arlington, NC

Received 18 August 2019, accepted 16 October 2019, DOI: 10.1111/php.13177

ABSTRACT

Ru(II) complexes were synthesized with π-expanding (phenyl, fluorenyl, phenanthrenyl, naphthalen-1-yl, naphthalene-2-yl, anthryl and pyrenyl groups) attached at a 1*H*-imidazo[4,5-*f*][1,10]phenanthroline ligand and 4,4′-dimethyl-2,2′-bipyridine (4,4′-dmb) coligands. These Ru(II) complexes were characterized by 1D and 2D NMR, and mass spectroscopy, and studied for visible light and dark toxicity to human malignant melanoma SK-MEL-28 cells. In the SK-MEL-28 cells, the Ru(II) complexes are highly phototoxic (EC_{50} = 0.2–0.5 μM) and have low dark toxicity (EC_{50} = 58–230 μM). The highest phototherapeutic index (PI) of the series was found with the Ru(II) complex bearing the 2-(pyren-1-yl)-1*H*-imidazo[4,5-*f*][1,10]phenanthroline ligand. This high PI is in part attributed to the π-rich character added by the pyrenyl group, and a possible low-lying and longer-lived ^{3}IL state due to equilibration with the ^{3}MLCT state. While this pyrenyl Ru(II) complex possessed a relatively high quantum yield for singlet oxygen formation (Φ_Δ = 0.84), contributions from type-I processes (oxygen radicals and radical ions) are competitive with the type-II ($^1O_2$) process based on effects of added sodium azide and solvent deuteration.

INTRODUCTION

A number of contributions have been made to understanding metal-organic dyad sensitizers in photodynamic therapy (PDT) and synergy in cancer cell killing (1–4), where ligand substitution on the metal serves to increase light absorption and triplet lifetime (5). In systems based on Ru(II) as well as other metals (6,7), excited states with intraligand (IL) character have been shown to increase the triplet lifetime (5). Whether these photosensitizers involve predominantly a type-II reaction producing $^1O_2$ as the key cytotoxic agent, or whether there is competition with the type-I reaction (oxygen radicals or radical ions) (8,9) has not been fully examined. It is plausible that both pathways contribute to the observed photocytotoxic effects due to the various types of excited states that are accessible in metal complexes (Fig. 1).

Depending on the nature of the metal complex, some of these excited state configurations include metal-to-ligand charge transfer (MLCT), metal centered (MC), metal-to-metal charge transfer (MMCT), in the case of multimetallic complexes, IL, intraligand charge transfer (ILCT) and ligand-to-ligand charge transfer (LLCT). We previously found that the ligand-centered (^{3}IL) state (10) in the π-expansive organic unit extended the triplet lifetime 10-fold due to an equilibrium with ^{3}MLCT state (11). When the energy of the ^{3}IL state is sufficiently low compared to the ^{3}MLCT state, its interaction with the ^{3}MLCT state becomes almost negligible, thereby forming a pure ^{3}IL state with an even longer lifetime. For example, a triplet lifetime of >100 μs was found by Kozlov et al. when pyrenylethynylene-conjugated bipyridine was incorporated in a Ru complex (12). In a similar vein, Ru(II) complexes that incorporated pyrenylethynylene conjugated to phenanthroline into the dyad were reported to extend the lifetime of the triplet state to 240 μs, which may be the longest lifetime reported to date for Ru complexes (13). Previous reports on Ru(II) dyads derived from 2,2′-bipyridine (bpy) and 4,4′-dimethyl-2,2′-bipyridine (4,4′-dmb) showed high phototoxicity with low dark toxicity (14,15), making these metal-organic dyads attractive photosensitizers for PDT.

In the present study, we explore complexes of the type $[Ru(4,4'\text{-dmb})_2(\text{ip-R})]^{2+}$, where imidazo[4,5-*f*][1,10]phenanthroline (ip) is fused to an aromatic R group. We hypothesized that increasing the π-conjugation in the R group will systematically lower the energy of the ^{3}IL state relative to the ^{3}MLCT state and thus improve phototoxic effects toward human melanoma SK-MEL-28 cells, particularly when the ^{3}IL energy drops below that of the ^{3}MLCT. The R groups investigated were as follows: 2-phenyl (**1**), 2-(9*H*-fluoren-2-yl) (**2**), 2-(phenanthrene-9-yl) (**3**), 2-(naphthalen-1-yl) (**4**), 2-(naphthalene-2-yl) (**5**), 2-(anthracene-10-yl) (**6**) and 2-(pyren-1-yl) (**7**) along with ruthenium 4,4′-dimethyl-2,2′-bipyridine (4,4′-dmb) coligands (Fig. 2). We determined whether complexes **1**-**7** (i) could be synthesized in high yield, (ii) would lead to high phototherapeutic indices (PI) in malignant melanoma SK-MEL-28 cells, (iii) would have high singlet oxygen quantum yields (Φ_Δ) and (iv) would show evidence in both type-I and type-II sensitized oxidation mechanisms. Our results have identified **7**, with pyrenyl as the R group, as a potentially useful photosensitizer against melanoma cells.

*Corresponding authors' emails: sherri.mcfarland@uta.edu (Sherri A. McFarland); agreer@brooklyn.cuny.edu (Alexander Greer)
†This article is part of a Special Issue dedicated to Dr. Jarod Finlay.

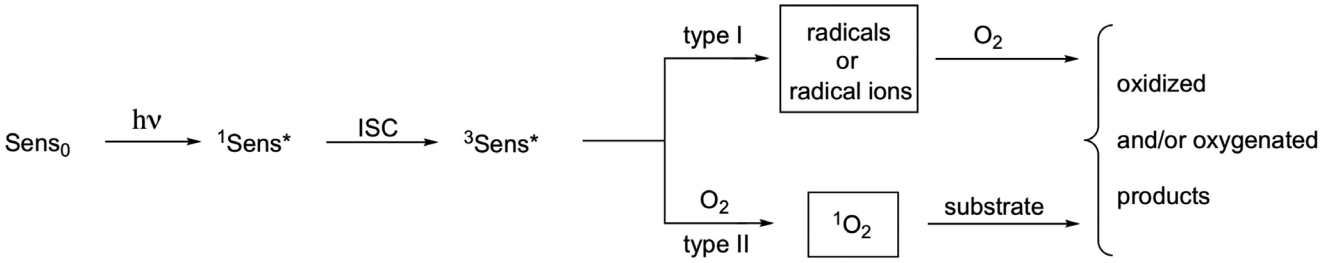

Figure 1. Type-I and type-II photosensitized oxidations. The type-I reaction forms oxygen radicals and radical ions, and the type-II reaction mainly forms singlet oxygen by energy transfer from an excited photosensitizer to triplet oxygen. Both reactions lead to oxidized and/or oxygenated products. Oxygenated products can include hydroperoxides and endoperoxides.

MATERIALS AND METHODS

Materials. 1,10-Phenanthroline-5,6-dione, NH_4OAC, glacial acetic acid, benzaldehyde, 9*H*-fluorene-2-carbaldehyde, phenanthrene-9-carbaldehyde, 1-napthaldehyde, 2-napthaldehyde, 9-anthraldehyde, pyrene-1-carbaldehyde, 9*H*-fluorene-2-carbaldehyde, phenanthrene-9-carbaldehyde, 4,4′-dimethyl-2,2′-bipyridine (4,4′-dmb), potassium nitrate (KNO_3), acetonitrile (MeCN), potassium hexafluorophosphate (KPF_6), dichloromethane (DCM), methanol (MeOH) and deuterated solvents (DMSO-d_6 and CD_3CN) were purchased from Sigma-Aldrich and used without further purification. Fetal bovine serum (FBS), RPMI 1640 (Corning Cellgro) and Eagle's minimum essential medium (EMEM) (Corning Cellgro) were purchased from VWR. Human malignant melanoma cells (SK-MEL-28) were obtained from the American Type Culture Collection (ATCC). Prior to use, FBS was divided into 40 mL aliquots, heat-inactivated (30 min, 55°C) and then stored at −20°C. Deionized water of 18 MΩ cm resistivity from a Barnstead filtration system was used for the biological experiments.

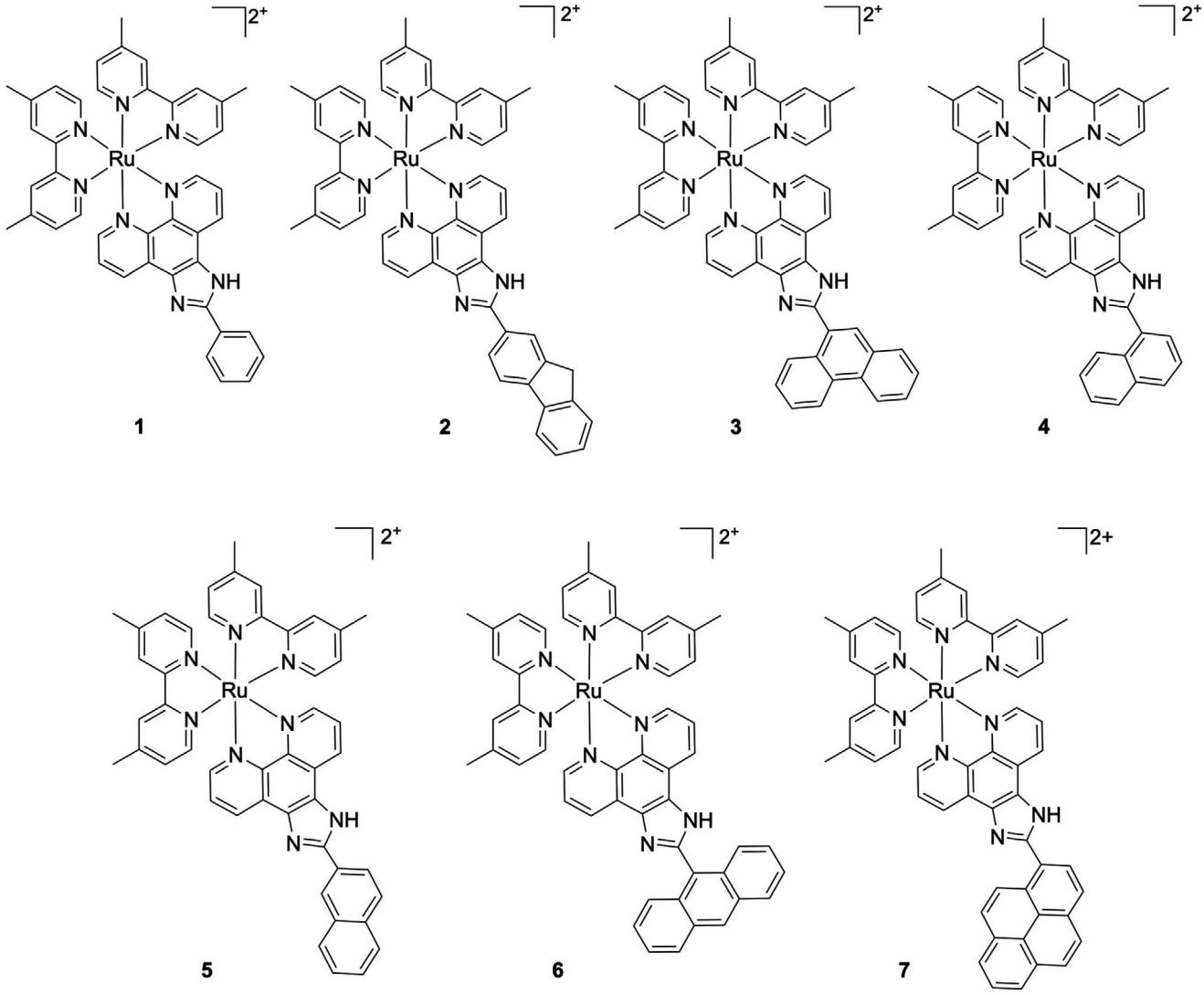

Figure 2. Structures of Ru(II) complexes **1**–**7** bearing functional ligands (ip-R).

Instrumentation. Microwave reactions were performed in a CEM Discover microwave reactor. NMR spectra were collected using Bruker AVANCE 500 (Dalhousie University Nuclear Magnetic Resonance Research Resource) or 300 MHz spectrometers (Acadia Centre for Microstructural Analysis), and ESI mass spectra were obtained using a Bruker microTOF focus mass spectrometer (Dalhousie University Mass Spectrometry Laboratory). HPLC analyses were performed with an Agilent 1100 series instrument (ChemStation Rev. A 10.02 software) using a Hypersil GOLD C18 reverse phase column with an A-B gradient (98% → 5% A; A = 0.1% formic acid in H_2O, B = 0.1% formic acid in MeOH).

Synthesis. The ligands 2-phenyl-1*H*-imidazo[4,5-*f*][1,10] phenanthroline (bip), 2-(naphthalen-1-yl)-1*H*-imidazo[4,5-*f*][1,10] phenanthroline (1-nip), 2-(naphthalen-2-yl)-1*H*-imidazo[4,5-*f*][1,10] phenanthroline (2-nip), 2-(9*H*-fluoren-2-yl)-1*H*-imidazo [4,5-*f*][1,10] phenanthroline (fip), 2-(pyren-1-yl)-1*H*-imidazo[4,5-*f*][1,10] phenanthroline (ippy) and 2-(anthracene-10-yl)-1*H*-imidazo[4,5-*f*][1,10] phenanthroline (aip) were synthesized according to literature procedures (16–21). Compounds $[Ru(4,4'\text{-dmb})_2Cl_2]\cdot 2H_2O$ (22), $Ru(4,4'\text{-dmb})_2(bip)](PF_6)_2$ **1** (23), $Ru(4,4'\text{-dmb})_2(ippy)](PF_6)_2$ **7** (24) and 9,10-anthracene dipropionate dianion **8** (25,26) were synthesized as reported in the literature. For our *in vitro* study, Ru(II) complexes **1**-**7** were converted to their corresponding Cl^- salts.

Synthesis of 2-(phenanthren-9-yl)-1H-imidazo [4,5-f][1,10] phenanthroline (pcip). Yield 247 mg (78%): purity >80%. A mixture of phen-dione (166.6 mg, 0.8 mmol), phenanthrene-9-carbaldehyde (165 mg, 0.8 mmol), NH_4OAC (1.23 g, 16 mmol) and glacial acetic acid (4 mL) was subjected to microwave irradiation for 15 min at 180°C. The resulting solution was diluted with water in a beaker, and ammonium solution was added dropwise until the pH of the solution reached 8. A yellow precipitate was formed, which was filtered through a fine glass-sintered frit. Single spot in TLC indicated pure product was formed. ^{1}H NMR (300 MHz, DMSO-d_6) δ 9.08 (d, J = 5.0 Hz, 2H; a,d), 8.99 (m, 4H; c,f,o,l), 8.48 (s, 1H; g), 8.19 (d, J = 7.7 Hz, 1H; k), 7.92–7.73 (m, 6H; b,e,n,m,i,j).

Synthesis of [Ru(4,4′-dmb)$_2$(fip)](PF$_6$)$_2$ 2. Yield 55 mg (48%): purity 98%. In a microwave vessel, 63.4 mg (0.11 mmol) of $[Ru(4,4'\text{-dmb})_2Cl_2]\cdot 2H_2O$ was mixed with 38.4 mg (0.10 mmol) of FIP. Ethylene glycol (3.0 mL) was added to the vessel. The mixture was microwaved for 15 min at 180°C. The resulting dark red color solution was directly loaded on to a silica column and eluted using 100% MeCN followed by 5% H_2O in MeCN to remove the excess starting material and other impurities. Finally, Ru(II) complex **2** was eluted as an orange band with 5–10% H_2O and 0.5–2.5% KNO_3 in MeCN to give an orange solid as a mixture of Cl^- and NO_3^- salts. This mixture was converted to the PF_6^- salt by adding 5–10 mL of water and 2–4 mL of saturated KPF_6. Evaporation of DCM under reduced pressure gave the pure PF_6^- salt as an orange solid: R_f = 0.51 (10% H_2O + 2.5% KNO_3 in MeCN). HPLC retention time: 25.6 min. ^{1}H NMR (300 MHz, acetonitrile-d_3) δ 9.00 (s, 2H; f, c), 8.52 (s, 1H; g), 8.40 (s, 2H; 3′), 8.36 (s, 2H; 3), 8.32 (s, 1H, n), 8.09 (d, J = 7.9 Hz, 1H; m), 8.04 (d, J = 5.2 Hz, 2H; a,d), 7.97 (d, J = 6.7 Hz, 1H; l), 7.79 (dd, J = 8.3, 5.2 Hz, 2H; b,e), 7.67 (m, 3H; 6′, i), 7.51 – 7.38 (m, 4H; 6, k, j), 7.30 (d, J = 5.8 Hz, 2H; 5′), 7.06 (d, J = 7.1 Hz, 2H; 5), 4.13 (s, 2H; h), 2.59 (s, 6H, 4′-Me), 2.48 (s, 6H, 4-Me). MS (ESI+) m/z: 999.13 $[M\text{-}PF_6]^+$, 853.47 $[M\text{-}PF_6\text{-}H]^+$, 427.40 $[M^-2PF_6]^{2+}$. HRMS (ESI+) m/z for $C_{50}H_{40}N_8Ru$: calcd 427.1209, found 427.1204.

Synthesis of [Ru(4,4′-dmb)$_2$(pcip)](PF$_6$)$_2$ 3. Yield 38 mg (33%): purity 98%. In a microwave vessel, 63.4 mg (0.11 mmol) of [Ru (4,4′-dmb)$_2$Cl$_2$]·2H$_2$O was mixed with 39.6 mg (0.10 mmol) of PCIP. Ethylene glycol (3.0 mL) was added to the vessel. The mixture was microwaved at 180°C for 15 min. The resulting dark red color solution was directly loaded on to a silica column and eluted using 100% MeCN followed by 5% H_2O in MeCN to remove the excess starting material and other impurities. Finally, Ru(II) complex **3** was eluted as an orange band with 5–10% H_2O and 0.5–2.5% KNO_3 in MeCN to give an orange solid as a mixture of Cl^- and NO_3^- salts. This mixture was converted to the PF_6^- salt by adding 5–10 mL of water and 2–4 mL of saturated KPF_6. Evaporation of DCM under reduced pressure gave the pure PF_6^- salt as an orange solid: R_f = 0.64 (10% H_2O + 2.5% KNO_3 in MeCN). HPLC retention time: 24.9 min. ^{1}H NMR (500 MHz, acetonitrile-d_3) δ 9.29 (d, J = 8.2 Hz, 1H; o), 9.10 (d, J = 8.2 Hz, 2H; f, c), 8.93 (d, J = 8.2 Hz, 1H; l), 8.86 (d, J = 8.4 Hz, 1H; k), 8.55 (s, 1H; g), 8.43 (s, 2H; 3′), 8.38 (s, 2H; 3), 8.15 (d, J = 7.8 Hz, 1H; h), 8.07 (dd, J = 5.2, 1.3 Hz, 2H; a, d), 7.87–7.75 (m, 6H; b, e, n, m, i, j), 7.71 (d, J = 5.7 Hz, 2H; 6′), 7.46 (d, J = 5.9 Hz, 2H; 6), 7.33 (dd, J = 6.4, 1.5 Hz, 2H; 5′), 7.10 (dd, J = 5.8, 1.5 Hz, 2H; 5), 2.61 (s, 6H; 4′-Me), 2.51 (s, 6H; 4-Me). MS (ESI+) m/z: 1011.00 $[M\text{-}PF_6]^+$, 865.33 $[M^-PF_6^-H]^+$, 433.33 $[M^-2PF_6]^{2+}$. HRMS (ESI+) m/z for $C_{51}H_{40}N_8Ru$: calcd 433.1209, found 433.1209.

Synthesis of [Ru(4,4′-dmb)$_2$(1-nip)](PF$_6$)$_2$ 4. Yield 44 mg (40%): purity 96%. In a microwave vessel, 63.4 mg (0.11 mmol) of $[Ru(4,4'\text{-dmb})_2Cl_2]\cdot 2H_2O$ was mixed with 34.63 mg (0.10 mmol) of 1-NIP. Ethylene glycol (3 mL) was added to the vessel. The mixture was microwaved for 15 min at 180°C. The resulting dark red color solution was directly loaded on to a silica column and eluted using 100% MeCN followed by 5% H_2O in MeCN to remove the excess starting material and other impurities. Finally, Ru(II) complex **4** was eluted as an orange band with 5–10% H_2O and 0.5–2.5% KNO_3 in MeCN to give an orange solid as a mixture of Cl^- and NO_3^- salts. This mixture was converted to the PF_6^- salt by adding 5–10 mL of water and 2–4 mL of saturated KPF_6. Evaporation of DCM under reduced pressure gave the pure PF_6^- salt as an orange solid: R_f = 0.53 (10% H_2O + 2.5% KNO_3 in MeCN). HPLC retention time: 23.7 min.[1] H NMR (500 MHz, acetonitrile-d_3) δ 9.18 (d, J = 8.6 Hz, 1H; m), 9.05 (s, 2H; c, f), 8.42 (s, 2H, 3′), 8.38 (s, 2H; 3), 8.18 (t, J = 10 Hz, 2H; g, i), 8.12–8.07 (m, 3H; k, a, d), 7.82 (dd, J = 8.3, 5.3 Hz, 2H; b, e), 7.77 (t, J = 10 Hz, 1H; h), 7.75–7.68 (m, 4H; 6′, l, j), 7.44 (d, J = 5.8 Hz, 2H; 6), 7.33 (dd, J = 6.4, 1.5 Hz, 2H; 5′), 7.08 (dd, J = 5.8, 1.4 Hz, 2H; 5), 2.61 (s, 6H; 4′-Me), 2.51 (s, 6H; 4-Me). MS (ESI+) m/z: 961.2 $[M\text{-}PF_6]^+$, 815.2 $[M\text{–}PF_6\text{–}H]^+$, 408.1 $[M\text{–}2PF_6]^{2+}$. HRMS (ESI+) m/z for $C_{47}H_{38}N_8Ru$: calcd 408.1131, found 408.1126.

Synthesis of [Ru(4,4′-dmb)$_2$(2-nip)](PF$_6$)$_2$ 5. Yield 50 mg (45%): purity 99%. In a microwave vessel, 63.4 mg (0.11 mmol) of [Ru(4, 4′-dmb)$_2$Cl$_2$]·2H$_2$O was mixed with 34.63 mg (0.10 mmol) of 2-NIP. Ethylene glycol (3 mL) was added to the vessel. The mixture was placed in a microwave for 15 min at 180°C. The resulting dark red color solution was directly loaded on to a silica column and eluted using 100% MeCN followed by 5% H_2O in MeCN to remove the excess starting material and other impurities. Finally, Ru(II) complex **6** was eluted as an orange band with 5–10% H_2O and 0.5–2.5% KNO_3 in MeCN to give an orange solid as a mixture of Cl^- and NO_3^- salts. This mixture was converted to the PF_6^- salt by adding 5–10 mL of water and 2–4 mL of saturated KPF_6. Evaporation of DCM under reduced pressure gave the pure PF_6^- salt as an orange solid: R_f = 0.58 (10% H_2O + 2.5% KNO_3 in MeCN). HPLC retention time: 24.4 min. ^{1}H NMR (500 MHz, acetonitrile-d_3) δ 9.05 (d, J = 8.2 Hz, 2H; c, f), 8.85 (d, J = 1.6 Hz, 1H; m), 8.45 (dd, J = 8.6, 1.8 Hz, 1H; g), 8.42 (s, 2H; 3′), 8.38 (s, 2H; 3), 8.17 (d, J = 8.7 Hz, 1H; h), 8.15–8.12 (m, 1H; l), 8.06 (dd, J = 5.2, 1.2 Hz, 2H; a, d), 8.05–8.03 (m, 1H; i), 7.82 (dd, J = 8.2, 5.3 Hz, 2H; b, e), 7.70–7.67 (m, 4H; 6′, j, k), 7.43 (d, J = 5.8 Hz, 2H; 6), 7.32 (dd, J = 6.1, 1.1 Hz, 2H; 5′), 7.07 (dd, J = 5.8, 1.0 Hz, 2H; 5), 2.61 (s, 6H; 4′-Me), 2.50 (s, 6H; 4-Me). MS (ESI+) m/z: 961.2 $[M^-PF_6]^+$, 815.3 $[M^-PF_6^-H]^+$, 408.1 $[M^-2PF_6]^{2+}$. HRMS (ESI+) m/z for $C_{47}H_{38}N_8Ru$: calcd 408.1131, found 408.1126.

Synthesis of [Ru(4,4′-dmb)$_2$(aip)](PF$_6$)$_2$ 6. Yield 64 mg (55%): purity 90%. In a microwave vessel, 63.4 mg (0.11 mmol) of [Ru(4, 4′-dmb)$_2$Cl$_2$]·2H$_2$O was mixed with 39.61 mg (0.10 mmol) of AIP. Ethylene glycol (3 mL) was added to the vessel. The mixture was microwaved for 15 min at 180°C. The resulting dark red color solution was directly loaded on to a silica column and eluted using 100% MeCN followed by 5% H_2O in MeCN to remove the excess starting material and other impurities. Finally, the desired Ru(II) complex was eluted as an orange band with 5–10% H_2O and 0.5–2.5% KNO_3 in MeCN to give an orange solid as a mixture of Cl^- and NO_3^- salts. This mixture was converted to the PF_6^- salt by adding 5–10 mL of water and 2–4 mL of saturated KPF_6. Evaporation of DCM under reduced pressure gave the pure PF_6^- salt as an orange solid: R_f = 0.48 (10% H_2O + 2.5% KNO_3 in MeCN). HPLC retention time: 24.0 min. ^{1}H NMR (500 MHz, acetonitrile-d_3) δ 8.88 (s, 1H; k), 8.44 (s, 2H; 3′), 8.40 (s, 2H; 3), 8.37 (d, J = 1.6 Hz, 1H; f), 8.32 (d, J = 1.6 Hz, 1H; c), 8.26 (d, J = 8.5 Hz, 2H; a, d), 8.11 (dd, J = 5.3, 1.3 Hz, 2H; o, l), 7.90 (t, J = 8.6 Hz, 1H; m), 7.85 (dd, J = 8.8, 1.1 Hz, 2H; g, j), 7.81 (t, J = 6.8 Hz, 1H; n), 7.73 (d, J = 5.7 Hz, 2H; 6′), 7.63 (m, 2H; b, e), 7.56 (m, 2H; h, i), 7.49 (d, J = 4.7 Hz, 2H; 6), 7.34 (dd, J = 5.7, 1.0 Hz, 2H; 5′), 7.14 (dd, J = 6.1, 1.2 Hz, 2H; 5), 2.62 (s, 6H; 4′-Me), 2.54 (s, 6H; 4-Me). MS (ESI+) m/z: 1011.2 $[M^-PF_6]^+$, 433.1 $[M^-2PF_6]^{2+}$. HRMS (ESI+) m/z for $C_{51}H_{40}N_8Ru$: calcd 433.1209, found 433.1204.

Cell assays for dark and phototoxicity. Solutions of the Ru(II) complexes were prepared as follows: 5 mM stock solutions of the Ru(II) chloride complexes were prepared in 10% DMSO-H_2O and stored at − 20°C prior to use. Dilutions of the stock solutions were carried out with Dulbecco's phosphate-buffered saline (DPBS) (pH = 7.4). The SK-MEL-28 cells were cultured according to the procedure described in the literature (27). Cell viability experiments were conducted in triplicate using a 96-well plate, which had 200 μL of DPBS buffer added. Aliquots (50 μL) of cells in the log phase (SK-MEL-28 cells: ~550 000 cells mL^{-1}) were transferred to the inner well containing 25 μL of warm culture medium. The plate was placed in a 5% CO_2 water-jacketed incubator at 37°C for 3 h to allow the cells to equilibrate. The Ru(II) complexes were diluted with DPBS several times and prewarmed at 37°C before adding 25 μL of aliquots of appropriate concentration to the cells. Ru(II) complexes **1**–**7** treated microplates were incubated under 5% CO_2 at 37°C for 16 h drug-to-light intervals. Control cells that are not treated with light were kept in the dark. Cells in the microplate, those receiving light treatment, were treated with visible light (400–700 nm, 34.2 mW cm^{-2}) using a 190 W BenQ MS 510 overhead projector for 49 min to apply the total light doses of 100 J cm^{-2}. Control cells and light-treated cell in the microplate both were kept inside the incubator for another 48 h. Then, 10 μL aliquots of Alamar blue was added to each well plate and incubated for another 15–16 h. Viability of the cells was quantified based on the fluorescence of Alamar blue dye that emits from live cells, whereas it does not fluoresce in dead cells. Fluorescence was quantified using a Cytofluor 4000 fluorescence microplate reader. Excitation filter and emission filter of the microplate reader were set in 530 ± 25 nm and 620 ± 40 nm, respectively. EC_{50} values of the dark toxicity and photocytotoxicity were derived from eq 1 from the dose–response curve of GraphPad Prism 6.0. The y_i and y_f represent the initial and final fluorescence signal intensities, respectively. EC_{50} values are reproducible within the range of ± 25% in the submicromolar, ±10% below 10 μM and ± 5% above 10 μM region. PIs were calculated from the ratio of the dark EC_{50}-to-light EC_{50} values.

Singlet oxygen quantum yield measurements. The quantum yields for $^1O_2$ production (Φ_Δ) were measured relative to $[Ru(bpy)_3](PF_6)_2$ according to Eq. 2 (see footnote '*' in Table 2), where I, A and η are the integrated emission intensity, the absorbance at the excitation wavelength and the refractive index of the solvent, respectively, in which the subscript 's' denotes the standard. The reference value for Φ_Δ used for $[Ru(bpy)_3](PF_6)_2$ was 0.56 in aerated MeCN (28).

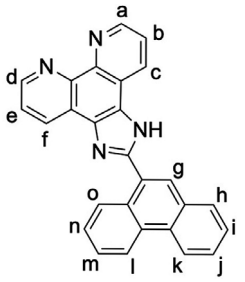

Figure 4. Proton NMR assignments of 2-(phenanthren-9-yl)-1*H*-imidazo [4,5-*f*][1,10]phenanthroline (pcip).

RESULTS AND DISCUSSION

Synthesis and characterization

A two-step synthesis was carried out to reach Ru(II) complexes **1**-**7** (Fig. 3). *Step 1:* 1,10-phenanthroline-5,6-dione reacted with NH_4OAc, in glacial acetic acid, and an appropriately substituted aldehyde under microwave irradiation at 180°C for 15 min to obtain ip–$R_{1\text{-}7}$ in 50–80% yields. *Step 2:* $[Ru(4,4'\text{-dmb})_2Cl_2]$ •$2H_2O$ reacted with ip–$R_{1\text{-}7}$ under microwave irradiation in ethylene glycol at 180°C for 15 min to obtain a crude chloride salt of Ru(II) complexes **1**-**7**. These chloride salts were purified by column chromatography using acetonitrile and water with KNO_3, which led to their isolation as mixtures of Cl^- and NO_3^- salts. The mixtures were then converted to the corresponding PF_6^-

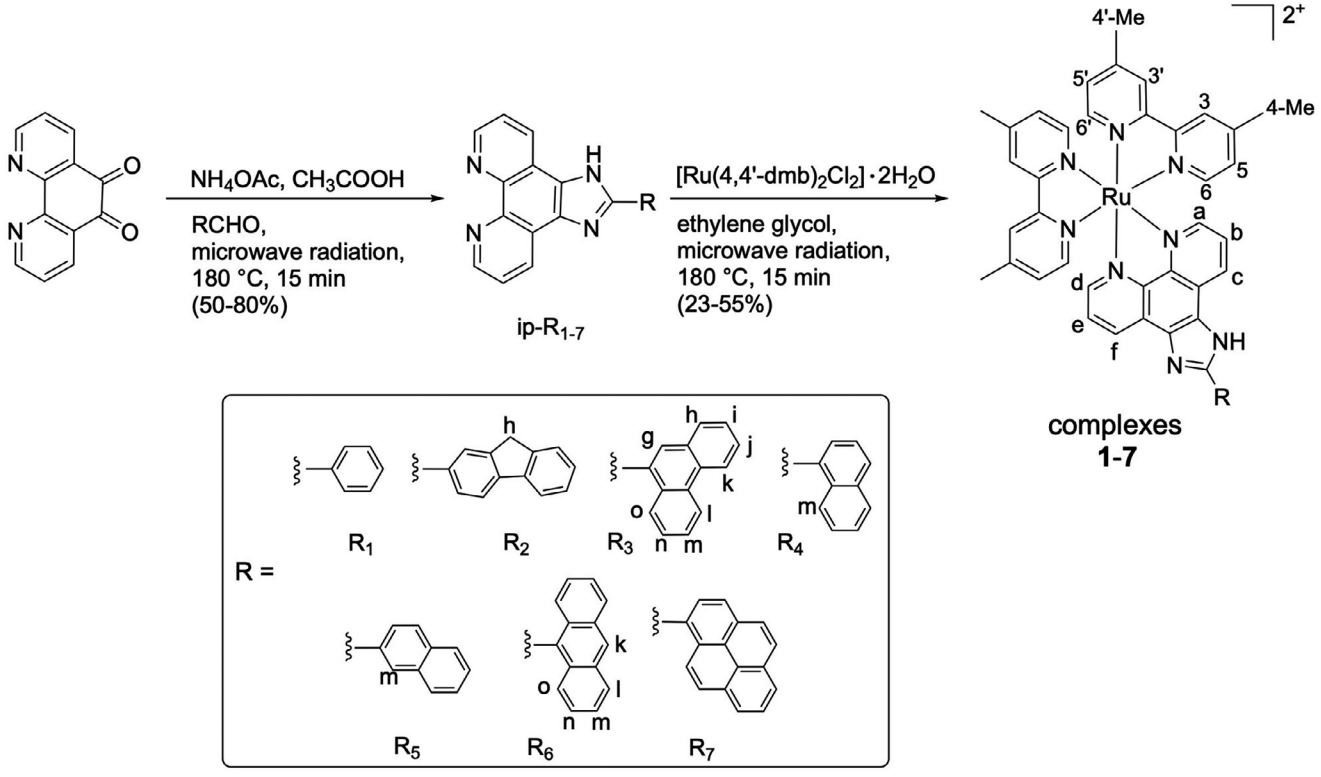

Figure 3. Two-step synthesis of Ru(II) complexes **1**-**7**.

Table 1. SK-MEL-28 cell photocytotoxicities of the new **Ru(II)** complexes **1**-**7** and Ru(II) complexes **8**-**11** previously reported in the literature

Ru(II) complexes	Dark EC_{50} (μM)*	Light EC_{50} (μM)*	PI†
1	143 ± 10	0.26 ± 0.01	558
2	82 ± 1	0.46 ± 0.02	179
3	59 ± 4	0.25 ± 0.01	232
4	133 ± 8	0.26 ± 0.04	505
5	96 ± 8	0.35 ± 0.02	277
6	98 ± 21	0.24 ± 0.01	409
7	230 ± 11	0.35 ± 0.02	657
8‡,§	>300	14.9 ± 0.2	>20
9‡,§	140 ± 10	0.07 ± 0.01	2071
10§	58.5 ± 0.5	0.35 ± 0.01	650
11¶	49.9 ± 0.3	0.125 ± 0.003	400

*Experiments were conducted in triplicate. Dark EC_{50} and light EC_{50} values were derived from Eq. 1 using a dose–response curve of GraphPad Prism 6.0, which are shown in the Supporting Information. $y = y_i + \frac{y_i - y_f}{1+10^{(\log EC_{50} - x)\times(\text{Hillslope})}}$. †Phototherapeutic indices (PIs) were calculated as the ratio of the dark EC_{50} and light EC_{50} values. ‡Ref. (30). §Ref. (31). ¶Ref. (32).

salts by introducing a saturated KPF_6 solution. The Ru(II) complexes **1**-**7** as PF_6^- salts were formed in 23–55% yields as red or orange solids.

Proton NMR assignments for the phenanthroline unit of ip have been reported earlier (27). However, 2-(phenanthren-9-yl)-1*H*-imidazo[4,5-*f*][1,10]phenanthroline (pcip) was not previously characterized. Here, we assign the pcip protons *a* and *d* as the most downfield protons because these are connected to a carbon which is directly attached to nitrogen (Fig. 4 and Figure S1). The close proximity to imidazolium nitrogen brings *f* and *c* signals downfield compared to the *b* and *e* signals. The singlet for *g* appeared at 8.48 ppm, and a doublet at 8.19 was tentatively assigned for *k*. Protons *b* and *e* appeared as a multiplet within 7.92–7.73 ppm. The other protons *o*, *l*, *n*, *m*, *i* and *j* appeared as a multiplet.

The characterization of Ru(II) complex **1** and **7** has been previously reported (27). Therefore, the characterization of Ru(II) complexes **2**-**6** is reported here. Based on HPLC data, the purity of **2** was 98%, of **3** was 98%, of **4** was 96%, of **5** was 99% and of **6** was 90%. The LCMS data indicated that **2** contained a fluorenyl group [(ESI+) *m/z* for $C_{50}H_{40}N_8Ru$: calcd 427.1209, found 427.1204], **3** contained a phenanthrenyl group [(ESI+) *m/z* for $C_{51}H_{40}N_8Ru$: calcd 433.1209, found 433.1209], **4** contained a naphthyl group [(ESI+) *m/z* for $C_{47}H_{38}N_8Ru$: calcd 408.1131, found 408.1126], **5** contained a naphthyl group [(ESI+) *m/z* for $C_{47}H_{38}N_8Ru$: calcd 408.1131, found 408.1126] and **6** contained an anthryl group [(ESI+) *m/z* for $C_{51}H_{40}N_8Ru$: calcd 433.1209, found 433.1204].

For Ru(II) complexes **1**–**7**, protons *c* and *f* in phenanthroline moiety were assigned as the most downfield protons at 9.13–8.89 ppm, because they are far from Ru electron cloud and

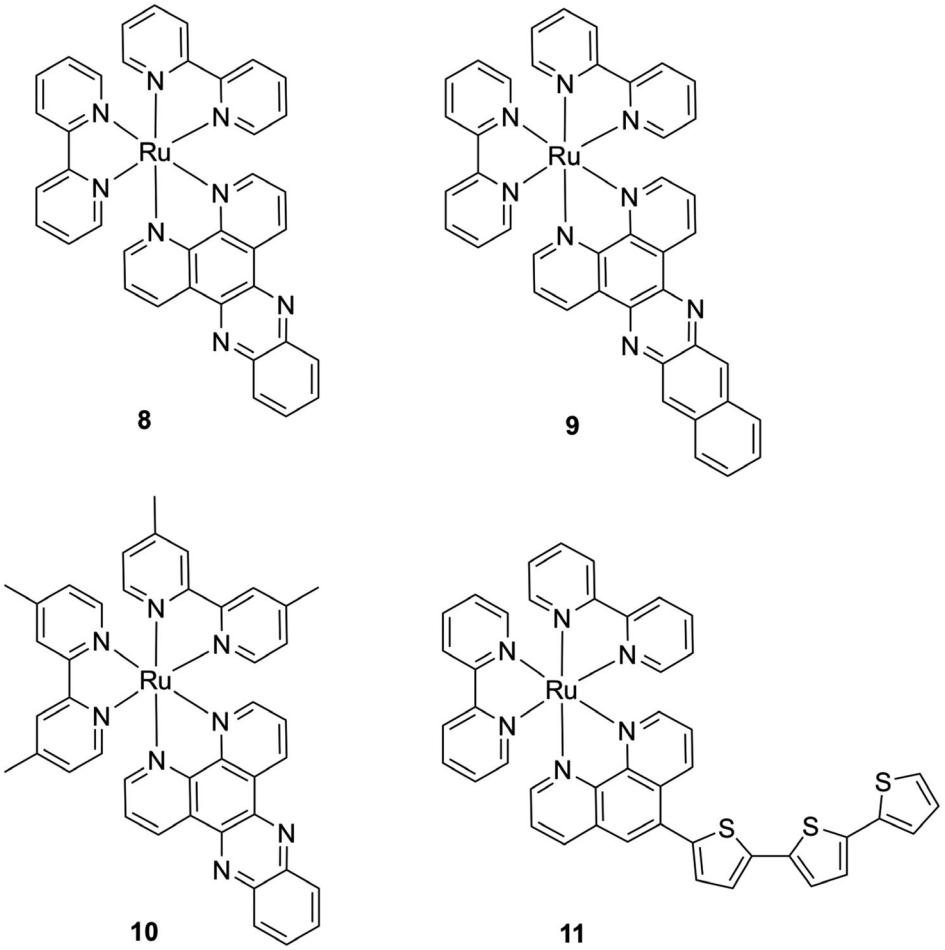

Figure 5. Structures of Ru(II) complexes **8**–**11**.

Table 2. Singlet oxygen quantum yields (Φ_Δ) for Ru(II) complexes **1-7** and literature triplet energies (E_T) of the π group (R_1-R_7) alone

Ru(II) complex	Φ_Δ*	π group (R_1–R_7) alone	E_T (eV)†
1	0.58	Benzene	3.66
2	0.59	Fluorene	2.92
3	0.60	Phenanthrene	2.69
4	0.69	Naphthalene	2.64
5	0.67	Naphthalene	2.64
6	0.87	Anthracene	1.82
7	0.84	Pyrene	2.08

*Singlet oxygen quantum yields (Φ_Δ) for **1-7** were measured in aerated acetonitrile using Eq. 2 relative to $[Ru(bpy)_3](PF_6)_2$ ($\Phi_\Delta = 0.57$ in aerated acetonitrile) (24,35) and contains ± 5% error. See Materials and Methods section for more information on the Φ_Δ measurement. $\Phi_s = \Phi_r \left(\frac{I_r}{A_r}\right)\left(\frac{A_s}{I_s}\right)\left(\frac{\eta_s^2}{\eta_r^2}\right)$. †$E_T$ values of benzene (36), fluorene, phenanthrene, naphthalene (37), pyrene (38) and anthracene (39) were obtained from the literature.

closer to imidazolium nitrogens (Figures S2–S7). However, the signals for *c* and *f* were slightly upfield shifted for **6** and appeared within 8.37–8.32 ppm. The protons *b* and *e* in phenanthroline moiety of complexes **1**–**7** that appeared within 7.93–7.63 ppm were assigned based on their correlation with *c* and *f*. For all complexes, *a* and *d* appeared as a doublet within 8.26–7.97 ppm. Downfield chemical shifts were observed for the aromatic protons attached to the 4,4′-dmb unit in the Ru(II) complexes in the following order: 3′,3 > 6′,6 > 5′,5 as reported previously in the literature (29). For **2**, methylene proton *h* appeared as a singlet at 4.14–4.13 ppm. Other aromatic protons on the fluorenone moiety of these complexes appeared in the range 8.55–7.38 ppm. Doublet for *m* attached to naphthalene chromophore in **5** appeared at 8.85 ppm, although this proton does not show an interaction with other protons in ^{1}H-^{1}H COSY, this doublet could be the result of long-range four bond coupling. A singlet for *g* in **3** appeared at 8.55 ppm, and indeed, all other aromatic protons of the phenanthrene unit in **3** appeared within 8.29–7.75 ppm. Protons *o*, *m* and *k* were assigned as the most downfield protons and appeared as doublet, doublet and singlet at 9.29 (for **3**), 9.18 (for **4**) and 8.88 ppm (for **6**), respectively. Protons *k* does not show correlation with another proton in **6,** whereas *o* and *m* showed correlation with *n* and *l*, respectively.

Table 3. H_2O/D_2O solvent and sodium azide quenching photochemical effects with Ru(II) complex **7** on the trapping of $^1O_2$ by anthracene **12**

Solvent	Yield **13** (μM)*	Yield **13** (μM)† (solvent+NaN3)	Ratio $\mathbf{13}_{D2O}/\mathbf{13}_{H2O}$	Ratio $\mathbf{13}_{D2O}/\mathbf{13}_{D2O+NaN3}$	Ratio $\mathbf{13}_{H2O}/\mathbf{13}_{H2O+NaN3}$
D_2O	28.1 ± 0.9	19.8 ± 1.0	2.0	1.5	0.80
H_2O	13.9 ± 3.7	16.7 ± 2.6			

*Irradiation (15 min) of a biphasic system containing 82 μM of **12** in D_2O or H_2O, and 63.7 μM of Ru(II) complex **7** in $CDCl_3$. †Endoperoxide **13** yield in presence of 1 mM sodium azide (NaN_3) added as a singlet oxygen quencher.

Photokilling of melanoma SK-MEL-28 cells

Table 1 and Figure S8 shows the phototoxic effects of Ru(II) complexes **1-7** in human malignant melanoma SK-MEL-28 cells. The cells were incubated with 1 nM to 300 μM complex **1-7** prior to irradiation with visible light (400-700 nm) in a 16 h drug-to-light interval. The phototoxicity results were obtained with a fluence of 100 J cm^{-2}, in which the highest concentration tested was 300 μM. Dark toxicities of Ru(II) complexes **1-7** were fairly low (ranging from 59 to 230 μM). We remind the reader that compounds with EC_{50} dark toxicities of >300 μM are generally considered to be nontoxic (4). In our case, the phototoxicities of Ru(II) complexes **1-7** were found to be in the tenths of micromolar range (0.24–0.46 μM). Ru(II) complex **7** had a particularly low dark toxicity and a fairly good phototoxicity resulting in the highest PI (of 657) in the series. The PI obtained for Ru(II) complex **6** is 409, which had an anthracene substituent. Subtle structural differences between naphth-1-yl and naphth-2-yl led to quite large differences in phototoxicities in the SK-MEL-28 cells, where the PI of **4** was about double that of **5**. The PI value for Ru(II) complex **1** was 558, which was second highest in the series. The relationship between the size of the substituent and phototoxicity of Ru(II) complexes **1-7** was only marginally correlated. For example, the pyrenyl-substituted Ru(II) complex **7** had a PI of only ~ 100 greater than the phenyl-substituted Ru (II) complex **1**. Another example is the slightly improved dark toxicity of **7** compared to **4**, where the phototoxicity is slightly better for **4** than **7**.

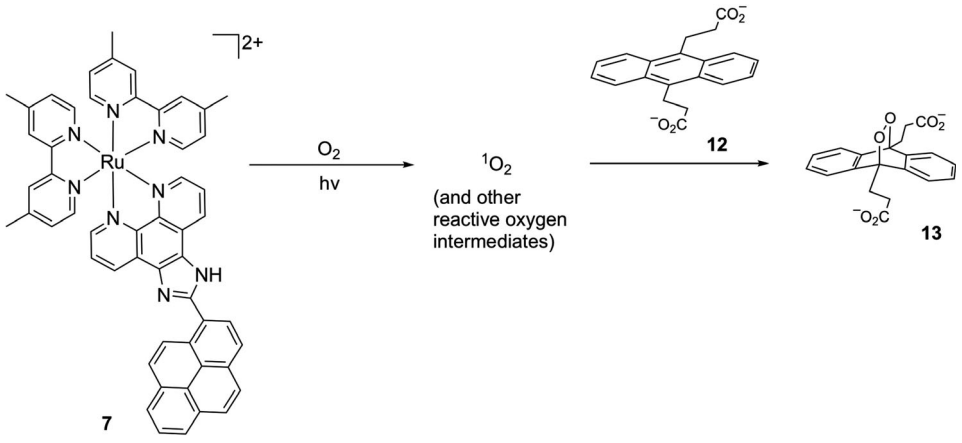

Figure 6. Reactive oxygen intermediates are generated by Ru(II) complex **7** upon illumination with white light in D_2O. The $^1O_2$ produced is detected by its reaction with 9,10-anthracene dipropionate dianion **12** to reach endoperoxide **13**.

We believe there is value in comparing the new Ru(II) complexes 1-7 to several Ru(II) complexes reported in the literature (31,32). However, we note that such a comparison of EC50 values in the literature run by another group using a different assay procedure is challenging. For example, EC50 values and PIs are often dependent on the assay protocol and cell line. Compounds **8**-**11** are Ru-based dyads containing π-expansive ligands combined with relatively small and substitutionally inert coligands bpy or 4,4′-dmb (Fig. 5). As seen in Table 1, changing either the coligand and/or the π-expansive functional ligand can have a marked effect on the dark and phototoxicities as well as the PIs, but not necessarily in a systematic way. Ru(II) complex **7** ranks among the least dark toxic in this comparison (surpassed only by **8**) and displays similar phototoxic effects as **10** and **11** (surpassed only by **9**). While its PI is not as large as that of **9**, the PI measured for **7** compares favorably with **10**, being among the two largest in the comparison. Ru(II) complex **7** does have a clear advantage over its counterpart with a similar PI in that **7** is almost four times less dark toxic, which is of consideration for a phototherapeutic agent.

Quantum yield for singlet oxygen formation (Φ_Δ)

Next, the singlet oxygen quantum yields for Ru(II) complexes **1**-**7** were measured. Table 2 shows that the Φ_Δ values ranged from a high of 0.87 for **6** to a low of 0.58 for **1**, which compare favorably to literature values for **8** (0.17) (30,31), **9** (0.79) (30,31), **10** (0.78) (31) and **11** (0.74) (32). For the new Ru(II) complexes, interestingly, we found that the quantum yields increase in the order **1** ≈ **2** ≈ **3** < **4** ≈ **5** < **6** ≈ **7** and very roughly correlate with the decrease of the triplet energies (E_T) of the π group (R_1–R_7) alone. The triplet energies of the π groups (R_1-R_7) are in the range of 3.66–1.82 eV. These π groups (R_1-R_7) decrease in the order benzene > fluorine > phenanthrene ≈ naphthalene > pyrene > anthracene. For comparison, to the π groups (R_1–R_7), the energy of the ^{3}MLCT state for $[Ru(bpy)_3]^{2+}$ complex is reported to be 2.1 eV (33). While the high Φ_Δ's for Ru(II) complexes **1**–**7** and low E_T's for the π groups (R_1–R_7) point to a type-II process, contributions from type-I processes may also exist, as was investigated next with Ru(II) complex **7**.

Mechanistic considerations

We next carried out experiments with Ru(II) complex **7** to assess whether its mechanism is dominated by type-I (oxygen radicals or radical ions) or type-II ($^1O_2$) processes. Data were collected with 9,10-anthracene dipropionate dianion **12** as a trapping agent for $^1O_2$ by a [4 + 2] cycloaddition reaction, in which the product of the trapping reaction is 9,10-endoperoxide **13** (Fig. 6) (25). Anthracene **12** has been used to verify the presence of $^1O_2$ in aqueous solution and is a good trapping agent based on a comparison to *trans*-2-methyl-2-pentenoate anion that undergoes an 'ene' reaction and is considered to be a fingerprint for $^1O_2$ (25,26). Here, anthracene **12** was used as it requires UV-vis instead of NMR and also a much lower concentration than the trans-2-methyl-2-pentenoate anion, another popular trap for $^1O_2$ detection. Our studies were carried out in H_2O or D_2O, and in the presence or absence of sodium azide (Table 3). We find that the efficiency of $^1O_2$ trapping by **12** increased by changing the solvent from H_2O and in D_2O. However, the increase in yield of endoperoxide **13** was two-fold in D_2O compared to H_2O. Because the lifetime of $^1O_2$ (τ_Δ) is 30-fold longer in D_2O *vs* H_2O (34), a greater difference in $^1O_2$ trapping in D_2O *vs* H_2O would have been expected if the Ru(II) complex **7** was mainly serving as a type-II sensitizer. We also found only a modest decrease in the $^1O_2$ trapping by **12** when sodium azide (a known $^1O_2$ quencher) was added to the reaction. Based on these results, we propose that Ru(II) complex **7** contains contributions from both type-I and type-II processes.

What are the mechanistic implications of these results?. Our finding for Ru(II) complex **7** is similar to an earlier study that showed Ru(II) complexes with α-oligothiophene groups contained contributions from both type-I and type-II processes (14). While type-I and type-II processes are oxygen dependent, contributions from Ru(II) complexes may also include oxygen-independent reactions. However in the current study, we did not explore the photokilling of the SK-MEL-28 cells under oxygen-free conditions to assess its potential contribution.

CONCLUSION

Herein, we report on Ru(II) dyads tethered to R groups that differ in π-conjugation in an attempt to increase the PI in a rational manner. Specifically, we synthesized Ru(II) complexes **1**-**7** by covalent attachment of phenyl, fluorenyl, phenanthrenyl, naphthalen-1-yl, naphthalene-2-yl, anthryl and pyrenyl groups to ip, which led to stable Ru(II) complexes **1**-**7**. These complexes were synthesized in modest yields (33–78%). As expected, the higher $^1O_2$ quantum yields roughly correlated with lower triplet state energies of the R groups. We found Ru(II) complex **7** to be the most promising dyad of the series, with a relatively high value for Φ_Δ (0.84) and a large PI toward SK-MEL-28 cells, which included contributions from both type-I and type-II processes based on the effects of added sodium azide and solvent deuteration.

Acknowledgements—Research reported in this publication was supported by the National Cancer Institute of the National Institutes of Health under Award Number R01CA222227 (to SAM). The content is solely the responsibility of the authors and does not necessarily represent the official views of the National Institutes of Health. SAM also acknowledges financial support from the University of North Carolina at Greensboro, the Natural Sciences and Engineering Council of Canada, the Canadian Institutes of Health Research, the Canadian Foundation for Innovation, the Nova Scotia Research and Innovation Trust, and Acadia University. GG, LL, and AG acknowledge support from the National Science Foundation (CHE-1856765). We thank Oliver Turque and Leda Lee for assistance with the table of contents graphic.

SUPPORTING INFORMATION

Additional supporting information may be found online in the Supporting Information section at the end of the article:

Figure S1. ^{1}H NMR spectrum of 2-(phenanthren-9-yl)-1*H*-imidazo [4,5-f][1,10] phenanthroline (pcip).

Figure S2. ^{1}H NMR spectrum (upper) and ^{1}H-^{1}H COSY spectrum (lower) of 1.

Figure S3. ^{1}H NMR spectrum of 2.

Figure S4. ^{1}H NMR spectrum (upper) and ^{1}H-^{1}H COSY spectrum (lower) of 3.

Figure S5. ^{1}H NMR spectrum (upper) and ^{1}H-^{1}H COSY spectrum (lower) of 4.

Figure S6. ^{1}H NMR spectrum (upper) and ^{1}H-^{1}H COSY spectrum (lower) of 5.

Figure S7. ^{1}H NMR spectrum (upper) and ^{1}H-^{1}H COSY spectrum (lower) of 6.

Figure S8. In vitro PDT dose response curves for Ru(II) complexes 1-7 in SK-MEL-28 cells.

REFERENCES

1. Sainuddin, T., M. Pinto, H. Yin, M. Hetu, J. Colpitts and S. A. McFarland (2016) Strained ruthenium metal–organic dyads as photocisplatin agents with dual action. *J. Inorg. Biochem.* **158**, 45–54.
2. Sgambellone, M. A., A. David, R. N. Garner, K. R. Dunbar and C. Turro (2013) Cellular toxicity induced by the photorelease of a caged bioactive molecule: Design of a potential dual-action Ru(II) complex. *J. Am. Chem. Soc.* **135**, 11274–11282.
3. Arenas, Y., S. Monro, G. Shi, A. Mandel, S. A. McFarland and L. Lilge (2013) Photodynamic inactivation of *Staphylococcus aureus* and methicillin-resistant *Staphylococcus aureus* with Ru(II)-based type I/type II photosensitizers. *Photodiagn. Photodyn. Ther.* **10**, 615–625.
4. Howerton, B. S., D. K. Heidary and E. C. Glazer (2012) Strained ruthenium complexes are potent light-activated anticancer agents. *J. Am. Chem. Soc.* **134**, 8324–8327.
5. Yin, H., M. Stephenson, J. Gibson, E. Sampson, G. Shi, T. Sainuddin, S. Monro and S. A. McFarland (2014) *In vitro* multiwavelength PDT with ^{3}IL states: Teaching old molecules new tricks. *Inorg. Chem.* **53**, 4548–4559.
6. Wang, L., S. Monro, P. Cui, H. Yin, B. Liu, C. G. Cameron, W. Xu, M. Hetu, A. Fuller, S. Kilina, S. A. McFarland and W. Sun (2019) Heteroleptic Ir(III)N_6 complexes with long-lived triplet excited states and *in vitro* photobiological activities. *ACS Appl. Mater. Interfaces* **11**, 3629–3644.
7. Liu, B., S. Monro, Z. Li, M. A. Jabed, D. Ramirez, C. G. Cameron, K. Colón, J. Roque, S. Kilina, J. Tian, S. A. McFarland and W. Sun (2019) New class of homoleptic and heteroleptic *bis*(terpyridine) iridium(III) complexes with strong photodynamic therapy effects. *ACS Appl. Bio. Mater.* **2**, 2964–2977.
8. Baptista, M. S., J. Cadet, P. Di Mascio, A. A. Ghogare, A. Greer, M. R. Hamblin, C. Lorente, S. C. Nunez, M. S. Ribeiro, A. H. Thomas, M. Vignoni and T. M. Yoshimura (2017) Type I and type II photosensitized oxidation reactions: Guidelines and mechanistic pathways. *Photochem. Photobiol.* **93**, 912–919.
9. Foote, C. S. (1991) Definition of type I and type II photosensitized oxidation. *Photochem. Photobiol.* **54**, 659–659.
10. Simon, J. A., S. L. Curry, R. H. Schmehl, T. R. Schatz, P. Piotrowiak, X. Jin and R. P. Thummel (1997) Intramolecular electronic energy transfer in ruthenium(II) diimine donor/pyrene acceptor complexes linked by a single C−C bond. *J. Am. Chem. Soc.* **119**, 11012–11022.
11. Ford, W. E. and M. A. J. Rodgers (1992) Reversible triplet-triplet energy transfer within a covalently linked bichromophoric molecule. *J. Phys. Chem.* **96**, 2917–2920.
12. Kozlov, D. V., D. S. Tyson, C. Goze, R. Ziessel and F. N. Castellano (2004) Room temperature phosphorescence from ruthenium(II) complexes bearing conjugated pyrenylethynylene subunits. *Inorg. Chem.* **43**, 6083–6092.
13. Lincoln, R., L. Kohler, S. Monro, H. Yin, M. Stephenson, R. Zong, A. Chouai, C. Dorsey, R. Hennigar, R. P. Thummel and S. A. McFarland (2013) Exploitation of long-lived ^{3}IL excited states for metal–organic photodynamic therapy: Verification in a metastatic melanoma model. *J. Am. Chem. Soc.* **135**, 17161–17175.
14. Shi, G., S. Monro, R. Hennigar, J. Colpitts, J. Fong, K. Kasimova, H. Yin, R. DeCoste, C. Spencer, L. Chamberlain, A. Mandel, L. Lilge and S. A. McFarland (2015) Ru(II) dyads derived from α-oligothiophenes: A new class of potent and versatile photosensitizers for PDT. *Coord. Chem. Rev.* **282–283**, 127–138.
15. Stephenson, M., C. Reichardt, M. Pinto, M. Wächtler, T. Sainuddin, G. Shi, H. Yin, S. Monro, E. Sampson, B. Dietzek and S. A. McFarland (2014) Ru(II) dyads derived from 2-(1-pyrenyl)-1*H*-imidazo[*4,5-f*][1,10]phenanthroline: Versatile photosensitizers for photodynamic applications. *J. Phys. Chem. A* **118**, 10507–10521.
16. Zhang, J., Q. Yu, Q. Li, L. Yang, L. Chen, Y. Zhou and J. Liu (2014) A ruthenium(II) complex capable of inducing and stabilizing BCL-2 G-quadruplex formation as a potential cancer inhibitor. *J. Inorg. Biochem.* **134**, 1–11.
17. Wang, J., S. Xu, F. Zhao, H. Xia and Y. Wang (2016) Computational and spectroscopic studies of the imidazole-fused phenanthroline derivatives containing phenyl, naphthyl, and anthryl groups. *J. Mol. Struct.* **1108**, 46–53.
18. Yi, X., J. Zhao, W. Wu, D. Huang, S. Ji and J. Sun (2012) Rhenium (I) tricarbonyl polypyridine complexes showing strong ab-sorption of visible light and long-lived triplet excited states as a triplet photosensitizer for triplet–triplet annihilation upconversion. *Dalton Trans.* **41**, 8931.
19. Shi, L. and B. Li (2009) A series of Cu(I) complexes containing 1,10-phenanthroline derivative ligands: Synthesis, characterization, photophysical, and oxygen-sensing properties. *Eur. J. Inorg. Chem.* **2009**, 2294–2302.
20. Zhong, R., S. Xu, J. Wang, F. Zhao, H. Xia and Y. Wang (2016) Experimental and theoretical investigations on spectroscopic properties of the imidazole-fused phenanthroline and its derivatives. *Spectrochim. Acta. A. Mol. Biomol. Spectrosc.* **161**, 27–32.
21. Mariappan, M. and B. G. Maiya (2005) Effects of anthracene and pyrene units on the interactions of novel polypyridylruthenium(II) mixed-ligand complexes with DNA. *Eur. J. Inorg. Chem.* **2005**, 2164–2173.
22. Sullivan, B. P., D. J. Salmon and T. J. Meyer (1978) Mixed phosphine 2,2′-bipyridine complexes of ruthenium. *Inorg. Chem.* **17**, 3334–3341.
23. Chao, H., R.-H. Li, Q.-W. Huang and L.-N. Ji (2002) Bis(4,4′-dimethyl-2,2′-bipyridine) ruthenium (II) complexes containing 2-arylimidazo-[4,5-*f*][1,10]phenanthroline: Syntheses, characterization and third-order nonlinear optical properties. *Chin. J. Chem.* **20**, 1235–1240.
24. Reichardt, C., M. Pinto, M. Wächtler, M. Stephenson, S. Kupfer, T. Sainuddin, J. Guthmuller, S. A. McFarland and B. Dietzek (2015) Photophysics of Ru(II) dyads derived from pyrenyl-substituted imidazo[4,5-*f*][1,10]phenanthroline ligands. *J. Phys. Chem. A* **119**, 3986–3994.
25. Aebisher, D., M. Zamadar, A. Mahendran, G. Ghosh, C. McEntee and A. Greer (2010) Fiber-optic singlet oxygen [$^{1}O_2$ ($^{1}\Delta_g$)] generator device serving as a point selective sterilizer. *Photochem. Photobiol.* **86**, 890–894.
26. Pushalkar, S., G. Ghosh, Q. Xu, Y. Liu, A. A. Ghogare, C. Atem, A. Greer, D. Saxena and A. M. Lyons (2018) Superhydrophobic photosensitizers: Airborne $^{1}O_2$ killing of an *in-vitro* oral biofilm at the plastron interface. *ACS Appl. Mater. Interfaces* **10**, 25819–25829.
27. Sainuddin, T., J. McCain, M. Pinto, H. Yin, J. Gibson, M. Hetu and S. A. McFarland (2016) Organometallic Ru(II) photosensitizers derived from π-expansive cyclometalating ligands: Surprising theranostic PDT effects. *Inorg. Chem.* **55**, 83–95.
28. DeRosa, M. C. and R. J. Crutchley (2002) Photosensitized singlet oxygen and its applications. *Coord. Chem. Rev.* **233**(234), 351–371.
29. Tan, L.-F., H. Chao, H. Li, Y.-J. Liu, B. Sun, W. Wei and L.-N. Ji (2005) Synthesis, characterization, DNA-binding and photocleavage studies of $[Ru(bpy)_2(PPIP)]^{2+}$ and $[Ru(phen)_2(PPIP)]^{2+}$. *J. Inorg. Biochem.* **99**, 513–520.
30. Chen, Y., W. Lei, G. Jiang, Q. Zhou, Y. Hou, C. Li, B. Zhang and X. Wang (2013) A ruthenium(II) arene complex showing emission enhancement and photocleavage activity towards DNA from singlet and triplet excited states respectively. *Dalton Trans.* **42**, 5924–5931.
31. Reichardt, C., S. Monro, F. H. Sobotta, K. L. Colon, T. Sainuddin, M. Stephenson, E. Sampson, J. III Roque, H. Yin, J. C. Brendel, C. G. Cameron, S. McFarland and B. Dietzek (2019) Predictive strength of photophysical measurements for *in vitro* photobiological activity in a series of Ru(II) polypyridyl complexes derived from π-Extended Ligands. *Inorg. Chem.* **58**, 3156–3166.
32. Monro, S., C. G. Cameron, X. Zhu, K. L. Colón, H. Yin, T. Sainuddin, M. Hetu, M. Pinto, A. Fuller, L. Bennett, J. III Roque, W. Sun and S. A. McFarland (2019) Synthesis, characterization, and photobiological studies of Ru(II) dyads derived from α-oligothiophene

derivatives of 1,10-phenanthroline. *Photochem. Photobiol.* **95**, 267–279.
33. Van Houten, J. and R. J. Watts (1976) Temperature dependence of the photophysical and photochemical properties of the tris(2,2′-bipyridyl)ruthenium(II) ion in aqueous solution. *J. Am. Chem. Soc.* **98**, 4853–4858.
34. Bartusik, D., D. Aebisher, A. M. Lyons and A. Greer (2012) Bacterial inactivation by a singlet oxygen bubbler: Identifying factors controlling the toxicity of $^1O_2$ bubbles. *Environ. Sci. Technol.* **46**, 12098–12104.
35. Ghosh, G., K. L. Colón, A. Fuller, T. Sainuddin, E. Bradner, J. McCain, S. M. A. Monro, H. Yin, M. W. Hetu, C. G. Cameron and S. A. McFarland (2018) Cyclometalated ruthenium (II) complexes derived from α-oligothiophenes as highly selective cytotoxic or photocytotoxic agents. *Inorg. Chem.* **57**, 7694–7712.
36. Shull, H. (1949) Vibrational analysis of the 3400 Å triplet-singlet emission of benzene. *J. Chem. Phys.* **17**, 295–303.
37. Ferguson, J., T. Iredale and J. A. Taylor (1954) The phosphorescene spectra of naphthalene and some simple derivatives. *J. Chem. Soc.* 3160–3165.
38. Evans, D. F. (1957) Perturbation of singlet–triplet transitions of aromatic molecules by oxygen under pressure. *J. Chem. Soc.* 1351–1357.
39. Padhye, M. R., S. P. McGlynn and M. Kasha (1956) Lowest triplet state of anthracene. *J. Chem. Phys.* **24**, 588–594.